



OPEN ACCESS

EDITED BY

Duane R. Wesemann,
Harvard Medical School, United States

REVIEWED BY

Richard L. Frock,
Stanford University, United States
Ming Tian,
Harvard Medical School, United States

*CORRESPONDENCE

Helen A. Beilinson
✉ beilinsonh@uchicago.edu

RECEIVED 27 November 2023

ACCEPTED 16 February 2024

PUBLISHED 05 March 2024

CITATION

Beilinson HA, Erickson SA and Golovkina T
(2024) The endogenous *Mtv8* locus
and the immunoglobulin repertoire.
Front. Immunol. 15:1345467.
doi: 10.3389/fimmu.2024.1345467

COPYRIGHT

© 2024 Beilinson, Erickson and Golovkina. This is an open-access article distributed under the terms of the [Creative Commons Attribution License \(CC BY\)](https://creativecommons.org/licenses/by/4.0/). The use, distribution or reproduction in other forums is permitted, provided the original author(s) and the copyright owner(s) are credited and that the original publication in this journal is cited, in accordance with accepted academic practice. No use, distribution or reproduction is permitted which does not comply with these terms.

The endogenous *Mtv8* locus and the immunoglobulin repertoire

Helen A. Beilinson^{1*}, Steven A. Erickson²
and Tatyana Golovkina^{1,3,4,5}

¹Department of Microbiology, University of Chicago, Chicago, IL, United States, ²Department of Immunobiology, Yale University, New Haven, CT, United States, ³Committee on Microbiology, University of Chicago, Chicago, IL, United States, ⁴Committee on Immunology, University of Chicago, Chicago, IL, United States, ⁵Committee on Genetics, Genomics and System Biology, University of Chicago, Chicago, IL, United States

The vast diversity of mammalian adaptive antigen receptors allows for robust and efficient immune responses against a wide number of pathogens. The antigen receptor repertoire is built during the recombination of B and T cell receptor (BCR, TCR) loci and hypermutation of BCR loci. V(D)J recombination rearranges these antigen receptor loci, which are organized as an array of separate V, (D), and J gene segments. Transcription activation at the recombining locus leads to changes in the local three-dimensional architecture, which subsequently contributes to which gene segments are utilized for recombination. The endogenous retrovirus (ERV) mouse mammary tumor provirus 8 (*Mtv8*) resides on mouse chromosome 6 interposed within the large array of light chain kappa V gene segments. As ERVs contribute to changes in genomic architecture by driving high levels of transcription of neighboring genes, it was suggested that *Mtv8* could influence the BCR repertoire. We generated *Mtv8*-deficient mice to determine if the ERV influences V(D)J recombination to test this possibility. We find that *Mtv8* does not influence the BCR repertoire.

KEYWORDS

endogenous retrovirus, immunoglobulin repertoire, V(D)J recombination, MTV, B cell receptor (BCR) repertoire

Introduction

The extensive diversity of the jawed vertebrate adaptive immune response depends on the programmed assembly and hypermutation of antigen receptor (AgR) genes (1). The first stage of AgR assembly is V(D)J recombination, initiated by lymphocyte-specific recombination activating genes 1 and 2 (RAG1 and RAG2), during which immunoglobulin (Ig) and T cell receptor (TCR) genes are recombined from discrete variable (V), diversity (D), and joining (J) gene segments (2).

AgR assembly is a sequential process during lymphocyte development. In B cells, the Ig heavy-chain (*Igh*) locus recombines in early and pro B cells prior to the kappa and lambda light chain (*Igk*, *Igl*) loci in pre B cells (2, 3). *Igh* recombines in two phases: first, D_H-to-J_H

rearrangements occur in lymphoid progenitors; second, V_H -to- DJ_H rearrangements occur in pro-B cells (2, 4). After successful (i.e. in-frame without premature stop codons) *Igh* recombination, *Igk* undergoes V_K -to- J_K recombination (3). If neither *Igk* allele successfully rearranges, the *Igl* locus recombines in a V_L -to- J_L fashion. During V(D)J recombination, RAG (a heterotetramer composed of RAG1 and RAG2 molecules) accumulates at recombination centers (RCs) that encompass J or DJ gene segments (for D-to-J/V-to-J and V-to-DJ recombination, respectively) (4). In RCs, RAG binds to a recombination signal sequences (RSS) that flanks the rearranging gene segment (4). Then, a partner RSS of the second gene segment is brought into the RC for synapsis and RAG-mediated cleavage.

V(D)J recombination determines the V, (D), and J gene segments used in a particular AgR gene and is dependent on three-dimensional chromosomal architecture. Specifically, V(D)J recombination is constrained to AgR loci by chromatin loops, the bases of which are defined by CCCTC-binding factor (CTCF)-bound CTCF-Binding Elements (CBEs) (5–9). The number of loops formed is dependent on the recombining locus (10). In addition to chromatin loops defining the AgR, chromosomal architecture also defines the mechanism by which recombining gene segments are brought into the RC (11).

The *Igk* locus is comprised of 92 functional (163 total) V_K and four functional J_K spread across 3.2 Mb (Figure 1A) and contracts into a recombination-competent chromosomal structure in developing pro- and pre-B cells (12, 13). Once contracted, the *Igk* locus forms a rosette-like structure with five V_K -containing loops and one loop with J_K and C_K gene segments (10). *Igk* rearrangement occurs predominantly through the collision of, and subsequent recombination between, the J_K -containing and a V_K -containing loop (10). While the *Igk* loops are thought to be predominantly shaped by the CBEs throughout the locus, it is unknown whether other factors are involved.

The endogenous retrovirus (ERV) mouse mammary tumor virus (MMTV), *Mtv8* was mapped to the *Igk* locus on chromosome 6 (Figure 1A) (14–16). *Mtv8* is a provirus with all open-reading frames (ORFs) intact, namely, *gag*, *pro*, *pol*, *env*, and

superantigen (SAG) (Figure 1B). The provirus does not produce infectious virions and is silent in the mammary glands, the targeted tissue of all MMTVs, potentially due to hypermethylation of its promoter region (17–19). The *Mtv8* SAG has a specificity for $V\beta 11$ and $V\beta 12$ (20). Mice strains harboring *Mtv8* lack $V\beta 11^+$ and $V\beta 12^+$ T cells (21), indicating that *Mtv8* is expressed in antigen presenting cells, such as dendritic cells and B cells which present SAG to cognate T cells (22). As *Mtv8* is mapped within the *Igk* locus, it was hypothesized that it may contribute to *Igk* recombination by driving high levels of transcription in its vicinity (23). It was suggested that recombination to the first V_K gene segment downstream of *Mtv8* ($V_K14-111$, formerly V_K9M) could allow for enhancer activation of the *Mtv8* promoter (23). To identify whether *Mtv8* affects the *Igk* repertoire, the frequency of recombination of the J_K gene segments to $V_K14-111$ was analyzed in inbred mouse strains with [BALB/c, C58.C, A/J, and C57BL/6J (B6J)] and without (C58, C.C58, NZB, and PERA/Ei) *Mtv8* (23). These experiments demonstrated that mice inheriting *Mtv8* have higher recombination between $V_K14-111$ and all J_K gene segments compared to strains without *Mtv8*. While these analyses suggested differences in the usage of $V_K14-111$, *Ig* repertoire comparisons between inbred mouse lines is not an ideal approach, as polymorphisms within the loci other than *Mtv8* could also influence the repertoires.

To address whether *Mtv8* shapes the repertoire of mice with this ERV, we used CRISPR/Cas9 technology to generate B6J mice lacking *Mtv8* and compared their *Ig* repertoire to that of wild-type (WT) B6J mice. We found that the absence of *Mtv8* had no significant effects on the *Igh*, *Igk*, and *Igl* gene segment usage. Thus, contribution of *Mtv8* to the mouse *Ig* repertoires can be definitively ruled out.

Methods

Mice

Mice utilized in this study were bred and maintained at the animal facility of The University of Chicago. The studies described

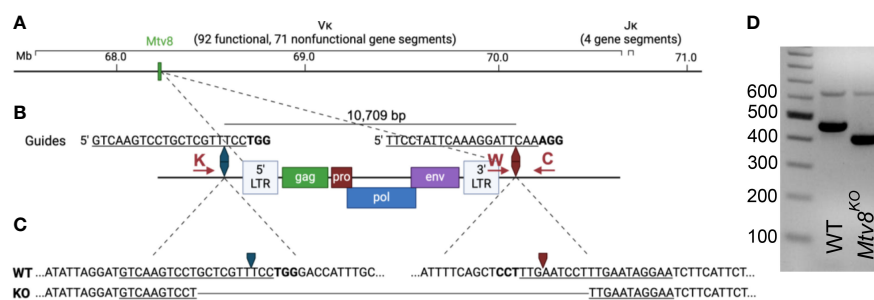


FIGURE 1

Generation of *Mtv8*^{KO} mice. (A) Schematic of B6J murine *Igk* locus on chromosome 6. Location of *Mtv8* is highlighted in green. (B) Schematic of *Mtv8* and guides used for CRISPR/Cas9 targeting of *Mtv8* to generate *Mtv8*^{KO} mice. LTR, long-terminal repeat; *gag*, group-specific antigen; *pro*, protease; *pol*, polymerase; *env*, envelope. Red arrows: genotyping primers (K: KOF, W: WTF, C: CommonR). (C) Genomic sequence of WT and KO *Mtv8* alleles. Only the flanking sequences are shown for the WT allele. For (B, C), underlined text indicates guide sequence, bold text indicates PAM sequence, arrows indicate Cas9-cut site. (D) Gel image of genotyping representative WT and homozygous *Mtv8*^{KO} mice. Mice were genotyped using a three-primer PCR with the KOF, WTF, and CommonR primers. WT product: 479 bp, KO product: 419 bp.

herein have been reviewed and approved by the Animal Care and Use Committee at the University of Chicago, which is accredited by the Association for Assessment and Accreditation of Laboratory Animal Care (AAALAC International).

C57BL/6J (B6J) mice were purchased from The Jackson Laboratory. *Mtv8*^{KO} B6J mice were generated using CRISPR/Cas9 technology. Two guide RNAs targeting the flanking up- and downstream sequences of *Mtv8* (5' guide: 5'-GTCAAGTCC TGCTCGTTTCC; 3' guide: 5'- TTCCTATTCAAAGGATTCAA) were co-injected into a single cell B6J embryos along with Cas9 (Figure 1B). Founder mice and subsequent offspring in which *Mtv8* was eliminated were identified using PCR with primers flanking the guide cut sites (KOF: 5'-GAATTTGGGTGCTCTTGCAT; CommonR: 5'-AACACAAATGGAGGCAAAGC; KO product size: 419 bp). To identify mice with the WT allele, a separate PCR was used using the CommonR primer and a WT-specific reverse primer that lies in the excited region (WTF: 5'- CAGTC CTAACATTCACCTCT; WT product size: 479 bp). A founder line was established in which *Mtv8* was eliminated with a 10,688 bp deletion (Figure 1C). The founder mouse was bred to a WT B6J mouse and the resulting F1 offspring were intercrossed to generate a homozygous KO line (Figure 1D). The deletion was confirmed at the DNA level by sequencing the KO allele using the KO-specific PCR primers.

RNA isolation from splenic B cells

CD19⁺ splenocytes were isolated from three WT and three *Mtv8*^{KO} 10.5-week-old B6J female mice. Red blood cell lysed splenocytes were labeled with microbeads conjugated to monoclonal anti-mouse CD19 antibodies (Miltenyi Biotec, Bergisch Gladbach, Germany) and positively sorted as detailed by the manufacturer. RNA was isolated from sorted cells using guanidine thiocyanate extraction and CsCl gradient centrifugation (24).

Library preparation

Immunoglobulin libraries were generated from 1 µg of RNA using the NEBNext Immune Sequencing Kit (New England Biolabs, Ipswich, Massachusetts, USA) according to manufacturer's instructions, specifically enriching for B cell receptor (BCR) chains during the first PCR step using the mouse NEBNext IS BCR primers included in the kit (Mus-IgGb: 5'-GATGGG GCTGTTGTTKTRGC; Mus-IgGa: 5'-GTGTCGTTTTGGCCTG; Mus-IgE: 5'-GGTTCCTGATAGAGGC; Mus-IgD: 5'- GTTCCTTTTTATCACC; Mus-IgM: 5'-TGACTCTC CTGMRGARAC; Mus-IgA: 5'-GTGGGTAGATGGTGGG; Mus-IgK: 5'-RCATCAGCCMGGTWT; Mus-IgL: 5'-ATGG HGWRGMCTTGGG). The libraries generated from the six individual mice were pooled in equimolar amounts and sequenced by paired-end 300 bp sequencing on an Illumina MiSeq by The University of Chicago Genomics Facility.

B cell receptor sequence processing and analysis

Preprocessing of BCR sequences was performed using the open-source workflow pRESTO NEBNext Immune Sequencing Kit Workflow (v3.2.0) on Galaxy (25). Reads with a Phred quality score <20 were removed for quality control. Reads that did not match to the constant region primer (maximum error rate 0.2) were removed. Reads that did not match to the template switch sequence (maximum error rate 0.5) were removed. The first 17 bp following the template switch site were a unique molecular identifier (UMI) on each read. Sequences with identical UMIs were collapsed into consensus sequences with sequences found in less than 60% of reads removed. Positions with more than 50% gap sequences were removed. Mate-pairs were assembled with a minimum of 8 bp overlap (maximum error rate of 0.3). Assembled reads were assigned isotype-constant region identities based on local alignment of the 3' ends of the reads (maximum error rate of 0.3). Using the *Mus musculus* reference C57BL/6J genome (GRCm38/mm10), V, (D), and J gene segments were assigned using MiGMAP mapper (Galaxy Version 1.0.3+galaxy2). Subsequent analyses were done using R Studio. Statistical significance was calculated using unpaired Welch's *t* test with Bonferroni correction. Graphing was done using GraphPad Prism version 10.0.1 for Mac (GraphPad Software, Boston, Massachusetts, USA).

Results

Generation of *Mtv8*-deficient B6J mice

Mtv8 knockout (KO) B6J mice were generated using a CRISPR/Cas9 approach. To target *Mtv8* without disturbing the V_K gene segments in its vicinity, we designed two guides to precisely delete the ERV: one 645 bp upstream of the 5' LTR and one 79 bp downstream of the 3' LTR (Figure 1B). A founder was identified using PCR with primers flanking the predicted deleted region and it was determined that a 10,688 bp deletion occurred, resulting in the elimination of the entire *Mtv8* locus (Figures 1C, D). The founder was crossed to a wildtype (WT) B6J mouse and heterozygous, mutant allele-carrying progeny were interbred to generate a homozygous *Mtv8*-deficient line (Figure 1D).

Mtv8 does not contribute to light and heavy chain recombination

To investigate whether *Mtv8* alters *Ig* gene segment usage, we analyzed the *Ig* repertoires of WT and *Mtv8*^{KO} B6J mice (Figures 2-4, Supplementary Table 1). Accordingly, RNA isolated from CD19⁺ splenocytes was used to prepare *Ig* heavy and light chain-specific 5'-RACE libraries, which were analyzed to determine the BCR repertoire using the pRESTO toolkit using the *Mus musculus* reference C57BL/6J genome (GRCm38/mm10) (25). The repertoire of productive transcripts was analyzed. Productive transcripts were defined as in-

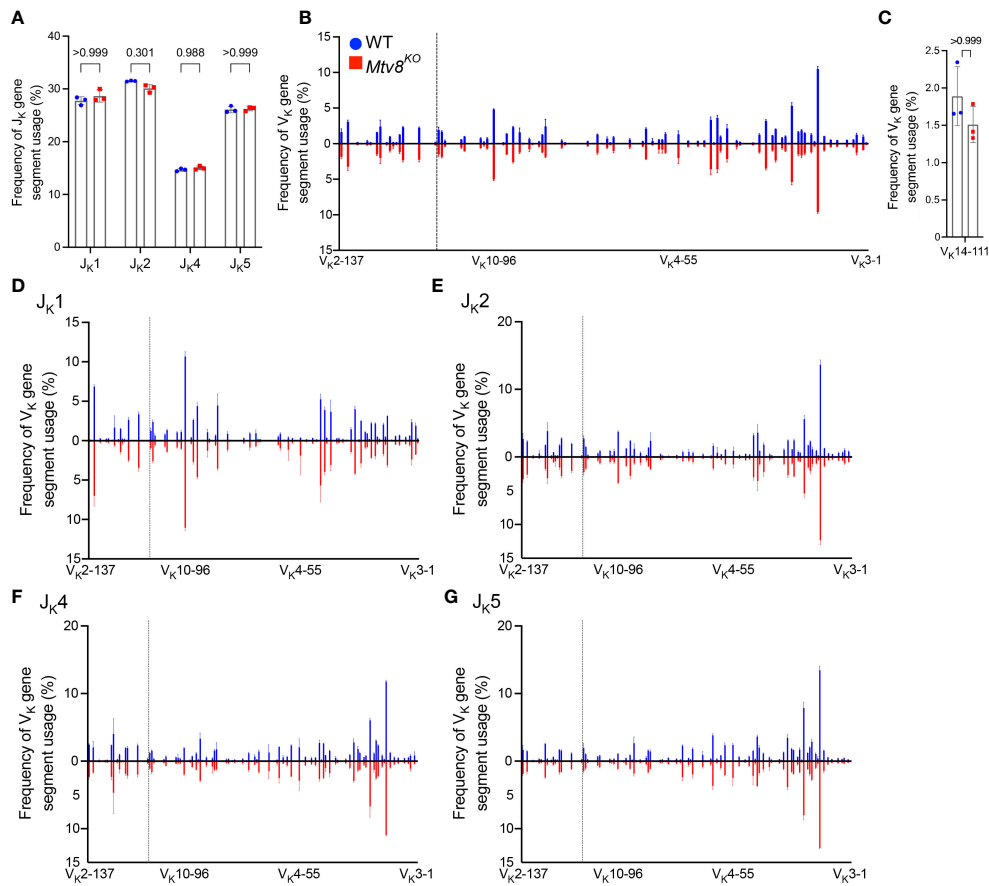


FIGURE 2

Igk repertoire of CD19⁺ splenocytes of *Mtv8*^{KO} mice. Frequency of J_K (A) and V_K (B) gene segments in productive *Igk* transcripts from CD19⁺ splenocytes. Productive recombination events are in-frame without premature stop codons. (C) Frequency of V_K14-111 (previously termed VK9M) in and productive *Igk* transcripts. (D-G) Frequency of V_K gene segments in total *Igk* transcripts recombined to J_K1 (D), J_K2 (E), J_K4 (F), and J_K5 (G). (B, D-G) V_K gene segments are arranged from 5' distal to 3' proximal to J_K gene segments and the vertical dotted line represents chromosomal location of *Mtv8*. n=3 mice per group. Data presented as mean with error bars indicated SD. Statistical significance was determined by unpaired Welch's *t* test with Bonferroni correction (numbers above bars indicate adjusted P value).

frame without premature stop codons and are likely those transcripts that are translated into expressed Ig proteins.

To determine whether *Mtv8* influences *Igk* recombination, we examined the J_K and V_K usage in productive *Igk* transcripts from CD19⁺ splenocytes (Figure 2). There was no difference in J_K usage (Figure 2A). Furthermore, the loss of *Mtv8* led to no alterations in the total V_K repertoire (Figure 2B). Notably, there was no change in usage of V_K gene segments mapped in the close proximity of *Mtv8* (dotted line; Figure 2B). An increased usage of the V_K gene segment, V_K14-111 (formerly called V_K9M) directly downstream of *Mtv8* in *Mtv8*⁺ mouse strains compared to *Mtv8*⁻ strains was previously reported (23). We observed no difference in frequency of V_K14-111 usage in *Igk* transcripts between WT and *Mtv8*^{KO} B6J mice (Figure 2C). Thus, the previously observed disparities in V_K14-111 usage between *Mtv8*⁺ and *Mtv8*⁻ mice from distinct genetic backgrounds are independent of *Mtv8*.

The same *Igk* locus can undergo multiple rounds of recombination. While *Mtv8* does not affect the overall frequency

of V_K usage, we wanted to test the possibility that it might affect either the first or subsequent recombination in distinct ways. Recombination of any V_K to J_K1 can only occur during a primary recombination event, as recombination to any other J_K gene segment would remove J_K1 from the *Igk* locus. Recombination to J_K2, J_K4, or J_K5 can either occur during a primary or secondary recombination event. As such, we calculated the frequency of V_K gene segment usage in total recombination events with each J_K gene segment. We found that, in line with globally unaffected J_K gene segment usage, frequency of any particular V_K gene segment recombining to J_K1, J_K2, J_K4, and J_K5 was unchanged with the loss of *Mtv8* (Figures 2D-G). Taken together, these data show that the *Igk* repertoire of *Mtv8*^{KO} B6J mice does not differ from WT B6J and that *Mtv8* does not influence the *Igk* recombination.

We also found no difference in the J_L and V_L usage among productive *Igl* transcripts between WT and *Mtv8*^{KO} B6J mice (Figure 3). Similarly, we found no alterations in J_H, D_H, and V_H gene segment usage between WT and *Mtv8*^{KO} mice (Figure 4).

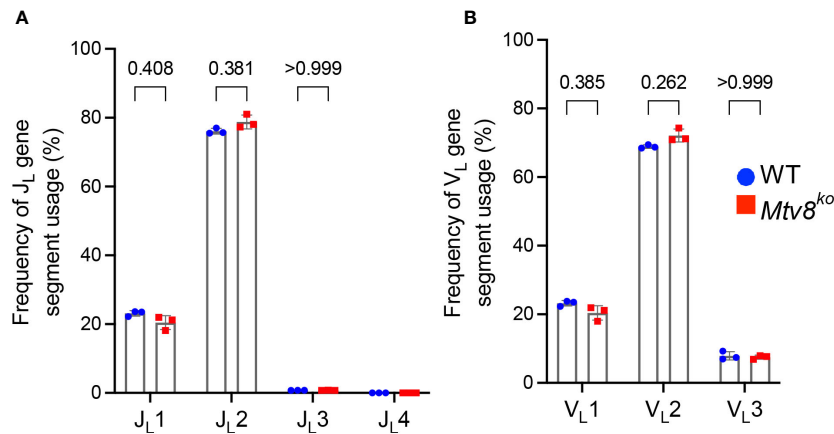


FIGURE 3
Igl repertoire of CD19⁺ splenocytes of *Mtv8*^{KO} mice. Frequency of J_L (A) and V_L (B) gene segments in and productive *Igl* transcripts from CD19⁺ splenocytes. Productive recombination events are in-frame without premature stop codons. n=3 mice per group. Data presented as mean with error bars indicated SD. Statistical significance was determined by unpaired Welch's *t* test with Bonferroni correction (numbers above bars indicate adjusted P value). No P value is indicated for JL4 as values for all samples are 0.

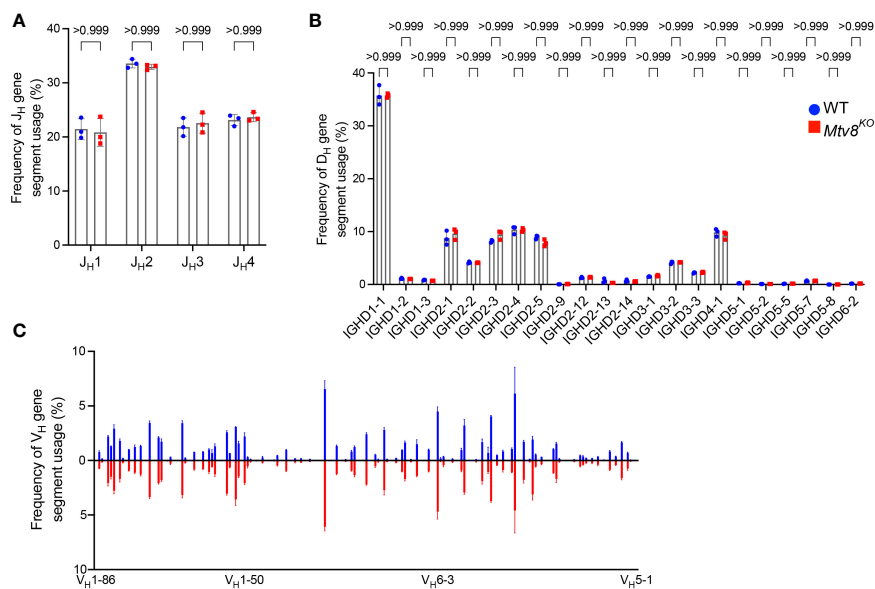


FIGURE 4
Igh repertoire of CD19⁺ splenocytes of *Mtv8*^{KO} mice. Frequency of J_H (A), D_H (B), and V_H (C) gene segments in productive *Igh* transcripts from CD19⁺ splenocytes. Productive recombination events are in-frame without premature stop codons. (B) D_H gene segments are arranged from 5' distal to 3' proximal to J_H gene segments. (C) Frequency of V_H gene segments in productive *Igh* transcripts that are statistically different between WT and *Mtv8*^{KO} mice. V_H gene segments are arranged from 5' distal to 3' proximal to D_H gene segments. n=3 mice per group. Data presented as mean with error bars indicated SD. Statistical significance was determined by unpaired Welch's *t* test with Bonferroni correction (numbers above bars indicate adjusted P value).

Discussion

It is now accepted that the collisions of the rosette-like loops of the *Igk* locus are the major mechanism of V_K-to-J_K recombination (10). However, the identification of an ERV, *Mtv8*, in the middle of the V_K array on the *Igk* locus led to the hypothesis that it may influence the *Ig* repertoire (14–16). Differences in V_K usage in mouse strains with and without *Mtv8* initially supported this

hypothesis (23). Now, advancements in genome-editing technologies allow us to definitely address whether a genetic loss of *Mtv8* can change the *Ig* repertoire within a mouse line. We show that *Mtv8* has no effect on the *Ig* repertoire by analyzing the *Igh*, *Igk*, and *Igl* transcriptional repertoires of B cells isolated from WT and *Mtv8*^{KO} B6J mice. These data demonstrate that while *Mtv8* is an intact ERV at the *Igk* locus, it has no influence on *Igk* recombination.

Data availability statement

The datasets presented in this study can be found in online repositories. The names of the repository/repositories and accession number(s) can be found below: <https://www.ncbi.nlm.nih.gov/geo/query/acc.cgi?acc=GSE248410>, GSE248410.

Ethics statement

The animal study was approved by University of Chicago Animal Resources Center. The study was conducted in accordance with the local legislation and institutional requirements.

Author contributions

HB: Conceptualization, Data curation, Formal analysis, Funding acquisition, Investigation, Methodology, Writing – original draft, Writing – review & editing. SE: Methodology, Writing – review & editing. TG: Funding acquisition, Methodology, Project administration, Resources, Supervision, Writing – review & editing.

Funding

The author(s) declare that no financial support was received for the research, authorship, and/or publication of this article.

Acknowledgments

We thank The University of Chicago Transgenic Mouse Facility (RRID:SCR_019171), especially Linda Degenstein, for

References

- Cooper MD, Alder MN. The evolution of adaptive immune systems. *Cell*. (2006) 124:815–22. doi: 10.1016/j.cell.2006.02.001
- Schatz DG, Swanson PC. V(D)J recombination: mechanisms of initiation. *Annu Rev Genet*. (2011) 45:167–202. doi: 10.1146/annurev-genet-110410-132552
- Alt FW, Zhang Y, Meng FL, Guo C, Schwer B. Mechanisms of programmed DNA lesions and genomic instability in the immune system. *Cell*. (2013) 152:417–29. doi: 10.1016/j.cell.2013.01.007
- Schatz DG, Ji Y. Recombination centres and the orchestration of V(D)J recombination. *Nat Rev Immunol*. (2011) 11:251–63. doi: 10.1038/nri2941
- Jhunjhunwala S, van Zelm MC, Peak MM, Murte C. Chromatin architecture and the generation of antigen receptor diversity. *Cell*. (2009) 138:435–48. doi: 10.1016/j.cell.2009.07.016
- Zhang Y, Zhang X, Dai HQ, Hu H, Alt FW. The role of chromatin loop extrusion in antibody diversification. *Nat Rev Immunol*. (2022) 22:550–66. doi: 10.1038/s41577-022-00679-3
- Davidson IF, Bauer B, Goetz D, Tang W, Wutz G, Peters JM. DNA loop extrusion by human cohesin. *Science*. (2019) 366:1338–45. doi: 10.1126/science.aaz3418
- Kim Y, Shi Z, Zhang H, Finkelstein JJ, Yu H. Human cohesin compacts DNA by loop extrusion. *Science*. (2019) 366:1345–9. doi: 10.1126/science.aaz4475
- Davidson IF, Peters JM. Genome folding through loop extrusion by SMC complexes. *Nat Rev Mol Cell Biol*. (2021) 22:445–64. doi: 10.1038/s41580-021-00349-7
- Hill L, Wutz G, Jaritz M, Tagoh H, Calderón L, Peters JM, et al. Igh and Igk loci use different folding principles for V gene recombination due to distinct chromosomal architectures of pro-B and pre-B cells. *Nat Commun*. (2023) 14:2316. doi: 10.1038/s41467-023-37994-9
- Zhang Y, Zhang X, Ba Z, Liang Z, Dring EW, Hu H, et al. The fundamental role of chromatin loop extrusion in physiological V(D)J recombination. *Nature*. (2019) 573:600–4. doi: 10.1038/s41586-019-1547-y
- Stadhouders R, de Bruijn MJW, Rother MB, Yuvaraj S, de Almeida CR, Kolovos P, et al. Pre-B cell receptor signaling induces immunoglobulin kappa locus accessibility by functional redistribution of enhancer-mediated chromatin interactions. *PLoS Biol*. (2014) 12:e1001791. doi: 10.1371/journal.pbio.1001791
- Roldan E, Fuxa M, Chong W, Martinez D, Novatchkova M, Busslinger M, et al. Locus 'decontraction' and centromeric recruitment contribute to allelic exclusion of the immunoglobulin heavy-chain gene. *Nat Immunol*. (2005) 6:31–41. doi: 10.1038/ni1150
- Robbins JM, Gallahan D, Hogg E, Kozak C, Callahan R. An endogenous mouse mammary tumor virus genome common in inbred mouse strains is located on chromosome 6. *J Virol*. (1986) 57:709–13. doi: 10.1128/jvi.57.2.709-713.1986

the generation of the *Mtv8*-deficient B6J mouse line. We thank The University of Chicago Genomics Facility (RRID:SCR_019196), especially Dr. Pieter Faber, for their assistance with sequencing Ig libraries. We thank Dr. Alexander Chervonsky for helpful discussions. We also thank Dr. David G. Schatz for advice and guidance on the project. This work was supported by The University of Chicago fund to T. G. and by the Duchossois Family Institute at the University of Chicago to H. A. B.

Conflict of interest

The authors declare that the research was conducted in the absence of any commercial or financial relationships that could be construed as a potential conflict of interest.

Publisher's note

All claims expressed in this article are solely those of the authors and do not necessarily represent those of their affiliated organizations, or those of the publisher, the editors and the reviewers. Any product that may be evaluated in this article, or claim that may be made by its manufacturer, is not guaranteed or endorsed by the publisher.

Supplementary Material

The Supplementary Material for this article can be found online at: <https://www.frontiersin.org/articles/10.3389/fimmu.2024.1345467/full#supplementary-material>

15. Yang JN, Boyd RT, Gottlieb PD, Dudley JP. The endogenous retrovirus Mtv-8 on mouse chromosome 6 maps near several kappa light chain markers. *Immunogenetics*. (1987) 25:222–7. doi: 10.1007/BF00404691
16. Yang JN, Dudley JP. The endogenous Mtv-8 provirus resides within the V kappa locus. *J Virol*. (1991) 65:3911–4. doi: 10.1128/jvi.65.7.3911-3914.1991
17. Golovkina TV. A novel mechanism of resistance to mouse mammary tumor virus infection. *J Virol*. (2000) 74:2752–9. doi: 10.1128/JVI.74.6.2752-2759.2000
18. Golovkina TV, Chervonsky A, Prescott JA, Janeway CA Jr., Ross SR. The mouse mammary tumor virus envelope gene product is required for superantigen presentation to T cells. *J Exp Med*. (1994) 179:439–46. doi: 10.1084/jem.179.2.439
19. Fanning TG, Morris DW, Cardiff RD, Bradshaw HD Jr. Characterization of an endogenous retrovirus-repetitive DNA chimera in the mouse genome. *J Virol*. (1985) 53:998–1000. doi: 10.1128/jvi.53.3.998-1000.1985
20. Holt MP, Shevach EM, Punksody GA. Endogenous mouse mammary tumor viruses (mtv): new roles for an old virus in cancer, infection, and immunity. *Front Oncol*. (2013) 3:287. doi: 10.3389/fonc.2013.00287
21. Dyson PJ, Knight AM, Fairchild S, Simpson E, Tomonari K. Genes encoding ligands for deletion of V beta 11 T cells cosegregate with mammary tumour virus genomes. *Nature*. (1991) 349:531–2. doi: 10.1038/349531a0
22. Acha-Orbea H, MacDonald HR. Superantigens of mouse mammary tumor virus. *Annu Rev Immunol*. (1995) 13:459–86. doi: 10.1146/annurev.iy.13.040195.002331
23. Yang JN, Dudley J. Endogenous Mtv-8 or a closely linked sequence stimulates rearrangement of the downstream V kappa 9 gene. *J Immunol*. (1992) 149:1242–51. doi: 10.4049/jimmunol.149.4.1242
24. Chirgwin JM, Przybyla AE, MacDonald RJ, Rutter WJ. Isolation of biologically active ribonucleic acid from sources enriched in ribonuclease. *Biochemistry*. (1979) 18:5294–9. doi: 10.1021/bi00591a005
25. Vander Heiden JA, Yaari G, Uduman M, Stern JNH, O'Connor KC, Hafler DA, et al. pRESTO: a toolkit for processing high-throughput sequencing raw reads of lymphocyte receptor repertoires. *Bioinformatics*. (2014) 30:1930–2. doi: 10.1093/bioinformatics/btu138